

# Adsorption of sulfur dioxide on Zircaloy-4 at 300 K

N. Stojilovic, J. D. Ehrman, and R. D. Ramsier<sup>a)</sup>

*Departments of Physics and Chemistry, The University of Akron, Akron, Ohio 44325-4001*

(Received 6 May 2005; accepted 30 January 2006; published 23 June 2006)

We investigate the interaction of sulfur dioxide (SO<sub>2</sub>) with Zircaloy-4 (Zry-4) surfaces after adsorption at 300 K. A shift in the Zr(*MNN*) feature toward lower energies of about 3 eV is observed following saturation exposures, indicating oxidation of Zr by dissociated oxygen. Temperature programmed desorption experiments indicate irreversible adsorption. Relatively short Ar-ion sputtering removes sulfur from the near-surface region without significantly affecting the oxygen Auger signal. Annealing of the SO<sub>2</sub>/Zry-4 system results in dissolution of oxygen into the bulk, leaving sulfur in the near-surface region. © 2006 American Vacuum Society.

[DOI: 10.1116/1.2180272]

## I. INTRODUCTION

Studies of the interaction of sulfur dioxide with surfaces of transition-metal oxides are relevant due to the role of sulfur as a poison for surface catalysis.<sup>1</sup> Also, sulfur dioxide pollutes the air and is considered as a health hazard. Some of the sources of SO<sub>2</sub> in the air are fossil-fuel combustion, industrial processes, volcanic gases, forest fires, and bacterial decay. The SO<sub>2</sub> from the atmosphere is responsible for acid rain that is known to be corrosive to metal and stone surfaces. The strong interaction of SO<sub>2</sub> upon adsorption is the result of a low-lying lowest unoccupied molecular orbital (LUMO) that makes the molecule an exceptional  $\pi$  acceptor. Dissociation of SO<sub>2</sub>, either spontaneous or thermally activated, is common for this molecule interacting with metal surfaces with the exception of Ag.<sup>2,3</sup>

Our motivation for studying the interaction of SO<sub>2</sub> with zirconium alloy is twofold. First, there are only a few ultrahigh vacuum (UHV) studies of the behavior of sulfur-containing species on zirconium surfaces. For example, 150 K adsorption of SO<sub>2</sub> on Zr(0001) using Auger electron spectroscopy (AES), temperature programmed desorption (TPD), and low-energy electron diffraction (LEED) was investigated in our laboratories,<sup>4</sup> whereas Wong and Mitchell<sup>5</sup> studied room temperature adsorption of H<sub>2</sub>S on Zr(0001) using LEED and AES methods. Second, the surface chemistry of zirconium alloys under ultrahigh vacuum conditions is much less studied than the surface chemistry of zirconium. Zircaloy-4 is nearly pure zirconium, containing more than 98% of the base metal. It is, therefore, also relevant to investigate how Zircaloy surface chemistry compares to that of zirconium.<sup>4</sup> Here, we investigate 300 K adsorption of SO<sub>2</sub> on Zry-4 using AES and TPD methods. Since TPD experiments show no desorption of species we will only present AES results.

## II. EXPERIMENT

Experiments were performed in an UHV system<sup>6</sup> at a base pressure of about  $3 \times 10^{-10}$  Torr. Exposure to SO<sub>2</sub> (Mathe-

son, 99.98%) was performed via a molecular beam doser whose design and calibration are described elsewhere.<sup>7</sup> Prior to each experiment the stainless steel gas-handling system was pumped with a turbomolecular pump. The elemental composition of Zry-4 in wt % is nominally 1.2%–1.4% Sn, 0.2% Fe, 0.2% Cr+O+Si, and the balance Zr. The Zry-4 sample was cut from sheet stock and had a surface area of 0.5 cm<sup>2</sup> and a thickness of 0.2 cm. Tantalum wires, spot welded to the sample, are used for direct current heating. A copper braid, connected to a liquid-nitrogen cold finger, is used for cooling the sample.

The surface was cleaned by sputtering and short annealing at ~920 K to dissolve traces of impurities such as oxygen or carbon, as confirmed using retarding-field AES operating at 3 keV. We do not detect any other compositional changes of the surface due to possible segregation during cleaning. Under these conditions the Sn(*MNN*)/Zr(*MNN*) ratio was below 0.12, as we recently reported.<sup>8</sup> The Auger signatures of other alloying elements are at the edge of the detection limits of our AES system. We do not observe significant electron beam effects on surface sulfur during AES and repeated scans show almost identical Auger spectra. During stepwise annealing experiments the sample temperature was increased at a rate of 1.8 K/s by resistive heating.

## III. RESULTS AND DISCUSSION

Figure 1 shows derivative mode Auger electron spectra of zirconium features as a function of SO<sub>2</sub> exposure at 300 K. The intensity of the overlapping Zr(*MNV*)+S(*LMM*) feature rapidly increases with SO<sub>2</sub> exposure up to about  $10.0 \times 10^{14}$ /cm<sup>2</sup> and appears to saturate at this point. The increase in the intensity of the Zr(*MNV*)+S(*LMM*) feature reflects an increase in sulfur content in the near-surface region. The vertical line is inserted to draw attention to the shift in the Zr(*MNN*) features. The shift of  $3(\pm 0.3)$  eV toward lower kinetic energies at saturation exposures reflects surface oxidation. Consistent with saturation in coverage, no further shift in this feature is observed above exposures of about  $10.0 \times 10^{14}$ /cm<sup>2</sup>. It is interesting that a shift of the Zr(*MNN*) feature of 3 eV was also observed after similar exposure of Zry-4 to oxygen at this temperature.<sup>9</sup> It is then obvious that

<sup>a)</sup>Author to whom correspondence should be addressed; electronic mail: rex@uakron.edu

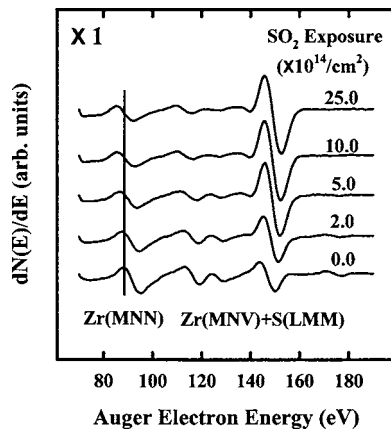


FIG. 1. Derivative mode AES spectra presenting zirconium and sulfur Auger transitions after various exposures to SO<sub>2</sub> at 300 K. The vertical line on the Zr(MNN) transition is inserted to stress the shift toward lower energies that directly reveals surface oxidation. The slight reduction of the Zr(MNN) feature following SO<sub>2</sub> adsorption is due to electron attenuation effects caused by the presence of sulfur and oxygen. The increase in the overlapping Zr(MNV)+S(LMM) feature is indicative of an increase in sulfur content. No further change in the zirconium oxidation state is observed above 10.0 × 10<sup>14</sup>/cm<sup>2</sup> exposures, which saturate the sulfur content.

near-surface sulfur does not prevent surface oxidation when a sufficient amount of oxygen is present. Even though sulfur reduced the amount of surface oxygen, it did not affect the zirconium (MNN) feature significantly.

Figure 2 shows the O(KLL) Auger features as a function of exposure. The same exposure sequence as shown in Fig. 1 is presented here. Rapid increase in the oxygen Auger signal that saturates at about 10.0 × 10<sup>14</sup>/cm<sup>2</sup> is evident. Our previous study of the <sup>18</sup>O<sub>2</sub>/Zry-4 system showed that notably greater exposures of about 100.0 × 10<sup>14</sup>/cm<sup>2</sup> were needed to saturate the near-surface region with oxygen.<sup>9</sup> Relatively short exposures that saturate the near-surface region after SO<sub>2</sub> adsorption can be rationalized by the presence of sulfur that occupy some of near-surface sites and are consistent with our study of 150 K adsorption of SO<sub>2</sub> on Zr(0001) surfaces.<sup>4</sup> We propose that after <sup>18</sup>O<sub>2</sub> adsorption on Zry-4

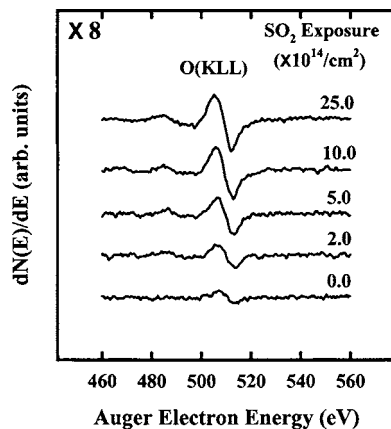


FIG. 2. Derivative mode AES spectra presenting the O(KLL) Auger transition after various exposures to SO<sub>2</sub> at 300 K. The surface saturates with oxygen by SO<sub>2</sub> exposures of about 10.0 × 10<sup>14</sup>/cm<sup>2</sup>.

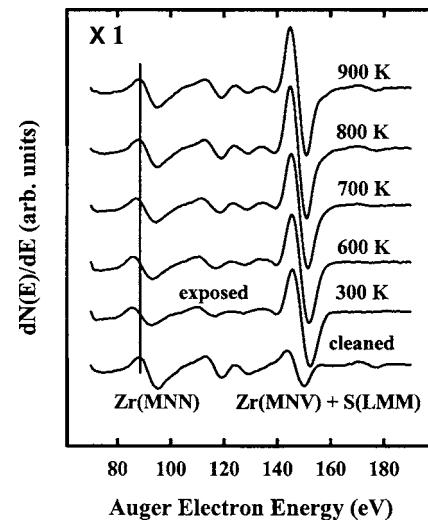


FIG. 3. AES spectra showing how SO<sub>2</sub> exposure (10.0 × 10<sup>14</sup>/cm<sup>2</sup>) and subsequent stepwise annealing change the zirconium and sulfur Auger transitions. Annealing to 600 K has no significant effect on surface oxide or on sulfur content. Annealing to 700 K shifts the Zr(MNN) feature toward higher energies, whereas annealing to 800 or 900 K completely removes the oxide film. Sulfur resides in the near-surface region at all temperatures.

that we studied earlier<sup>9</sup> oxygen dissociates and dissolves into the substrate, whereas here, after SO<sub>2</sub> adsorption, sulfur prevents oxygen dissolution which explains significantly lower saturation exposures in the presence of sulfur. Oxidation of Zry-4 surfaces by SO<sub>2</sub> chemisorption is interesting when one considers the fact that preexisting surface sulfur delays surface oxidation by adsorbing oxygen.<sup>10</sup>

Figure 3 shows derivative mode Auger electron spectra taken after cleaning, exposure to SO<sub>2</sub> (10.0 × 10<sup>14</sup>/cm<sup>2</sup>) at 300 K, and stepwise annealing from 600 to 900 K. After adsorption of SO<sub>2</sub> the Zr(MNN) shifts by about 3 eV toward lower kinetic energies and does not change even after annealing to 600 K. However, note that annealing to 700 K results in shift in the Zr(MNN) peak toward higher kinetic energies by about 1.5 eV, whereas annealing to 800 K completely removes the oxide layer, with the position of the Zr(MNN) transition returning to its clean surface value. An apparent increase in the intensities of the Zr(MNV)+S(LMM) and Zr(MNN) features after annealing to 800 or 900 K is a result of oxygen diffusion into the bulk at these temperatures. However, after SO<sub>2</sub> exposure the [Zr(MNV)+S(LMM)]/Zr(MNN) Auger peak-to-peak height ratios do not change significantly in stepwise annealing experiments.

Figure 4 shows the O(KLL) Auger signal during the same stepwise annealing sequence. Note that annealing to 600 K leaves the oxide layer intact and does not significantly change the intensity of the O(KLL) signal. Annealing to 700 K results in a shift of the Zr(MNN) feature by about 1.5 eV toward higher kinetic energies (Fig. 3) and also results in partial removal of oxygen from the surface (Fig. 4). We propose dissolution of oxygen into the bulk rather than desorption as a pathway for oxygen removal at higher temperatures. This is consistent with our TPD experiments that showed no desorption of oxygen-containing species in sig-

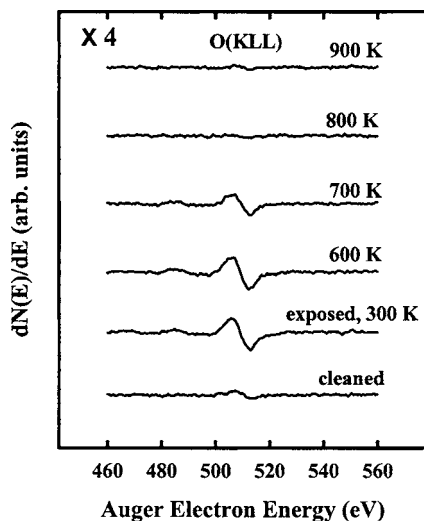


FIG. 4. AES spectra showing how  $\text{SO}_2$  exposure and subsequent stepwise annealing change the  $\text{O}(KLL)$  Auger transition. Annealing to 600 K has no significant effect on oxygen content in the near-surface region. Annealing to 700 K partly reduces the amount of oxygen, whereas annealing to 800 or 900 K completely dissolves the remaining oxygen into the bulk.

nificant amounts. Similar dissolution of oxygen in the presence of sulfur was observed for the  $\text{SO}_2/\text{Zr}(0001)$  system.<sup>4</sup> Note that annealing to 800 K seems to completely remove oxygen from the surface. We point out here that when no significant amount of sulfur resides near the surface, temperatures higher than 800 K are required to completely dissolve oxygen.

Impurities such as oxygen and carbon can be removed from the surface of zirconium and its alloys by annealing to high temperatures. Sulfur impurities, on the other hand, segregate from the bulk at higher temperatures and for removal require sputtering. It is important therefore to investigate how sputtering removes sulfur from the near-surface region. Figure 5 shows zirconium and sulfur Auger features following Zry-4 exposure to  $\text{SO}_2$  ( $20.0 \times 10^{14}/\text{cm}^2$ ) (a) and subsequent Ar-ion sputtering of 1 min (b), 2 min (c), and after annealing to 920 K (d). The ion beam energy was 2 keV and the sample current was kept near  $8 \mu\text{A}$ . Note that even relatively short sputtering times of only a few minutes notably reduce the  $[\text{Zr}(MNV)+\text{S}(LMM)]/\text{Zr}(MNN)$  ratio, reflecting the removal of sulfur from the surface region. A shift of the  $\text{Zr}(MNN)$  feature by  $1.2(\pm 0.3)$  eV toward higher energies is observed after 2 min of sputtering. This shift reflects ion beam effects on the surface oxide. Annealing to high temperatures then dissolves oxygen and returns some sulfur from beneath the surface to the near-surface region, thus making the surface even more contaminated with sulfur.

Prior to our  $\text{SO}_2$  experiments on Zry-4 we investigated segregation of bulk sulfur to the near-surface region and reported that prolonged annealing at high temperature is required to induce significant sulfur segregation.<sup>8</sup> We conclude that the increase in the  $\text{Zr}(MNV)+\text{S}(LMM)$  feature after quick annealing to 920 K, Fig. 5(d), originates from adsorbed sulfur rather than impurity bulk sulfur always present in transition metals. Our observations indicate that even

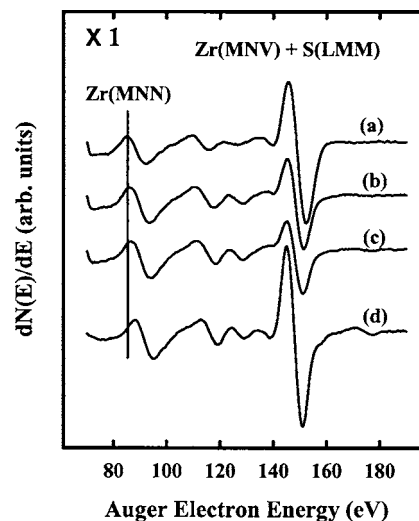


FIG. 5. AES data showing zirconium and sulfur features after a  $\text{SO}_2$  exposure of  $20.0 \times 10^{14}/\text{cm}^2$  (a) and after subsequent 2 keV Ar-ion sputtering for 1 min (b) and 2 min (c). Annealing to 920 K (d) brings sulfur back to the surface.

though relatively short sputtering times are sufficient for the removal of sulfur from the near-surface region, annealing returns dissolved sulfur to the surface that might play an important role in subsequent surface processes during heating. For example, it was reported that even small amounts of sulfur on  $\text{Cu}(111)$  drastically change the TPD spectra of  $\text{SO}_2$ .<sup>11</sup>

Figure 6 reveals how 2 keV Ar-ion sputtering affects the main oxygen Auger signal. It is interesting that the  $\text{O}(KLL)$  peak is only slightly reduced after 2 min sputtering (c). Annealing to 920 K appears to completely remove oxygen from the surface. We can now propose that due to this dissolution of oxygen into the bulk we observe an increase in absolute intensities of zirconium features after annealing to 920 K (d)

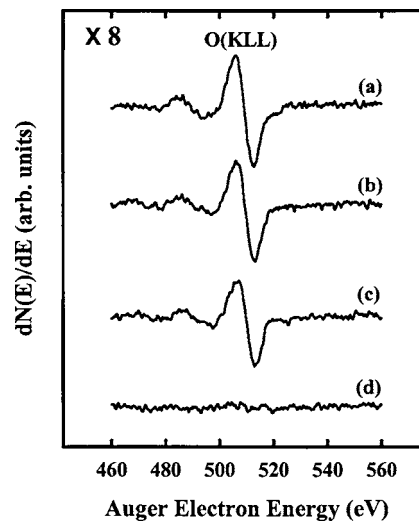


FIG. 6. AES data showing the  $\text{O}(KLL)$  Auger signal after a  $\text{SO}_2$  exposure of  $20.0 \times 10^{14}/\text{cm}^2$  (a) and after subsequent 2 keV Ar-ion sputtering for 1 min (b) and 2 min (c). Annealing to 920 K completely dissolves oxygen into the bulk (d).

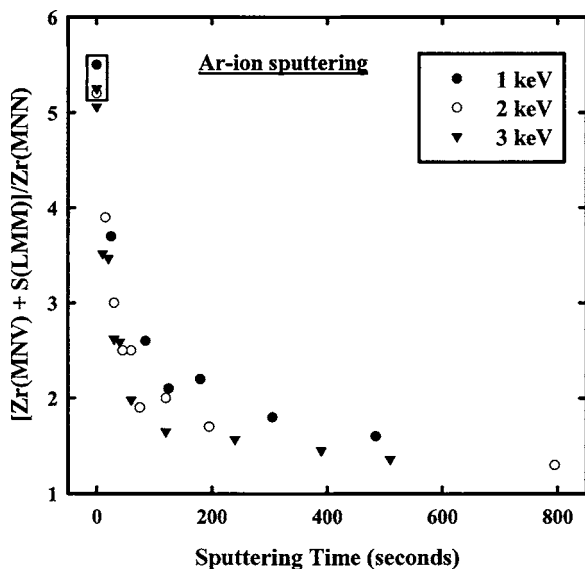


FIG. 7.  $[Zr(MNV)+S(LMM)]/Zr(MNN)$  Auger peak-to-peak height ratio as a function of sputtering time following exposure to  $20.0 \times 10^{14}/\text{cm}^2$  of  $\text{SO}_2$ . Ar-ion beam energies of 1, 2, and 3 keV were used. The sample current was kept near  $8 \mu\text{A}$ .

with respect to the surface probed just after  $\text{SO}_2$  adsorption (a). It is not surprising that in our sputtering experiments some sulfur was pushed beneath the surface since our ion beam is orthogonal to the surface of the sample. It is interesting that only the sulfur atoms are affected significantly in these short time intervals. Theoretical<sup>12</sup> and experimental<sup>13</sup> studies show that oxygen prefers octahedral subsurface sites. It is possible that oxygen predominantly occupies sites beneath the surface and is not easily accessed by direct ion collision. Also, greater atomic size of sulfur compared to oxygen makes the sulfur more likely a target for incoming Ar ions.

Different research groups studied surfaces of zirconium employing Ar-ion bombardment as part of a cleaning procedure at different kinetic energies. For example, for cleaning  $\text{Zr}(0001)$  we used 2 keV Ar-ion beam energy,<sup>4</sup> whereas 1 keV (Ref. 14) and 3 keV (Ref. 15) were also used by others. It is therefore relevant to investigate the effect of Ar-ion beam energy on the removal of sulfur from the near-surface region, especially since sulfur is an impurity that cannot be removed by annealing, as is the case with oxygen and carbon. Figure 7 shows how, following  $\text{SO}_2$  adsorption ( $20.0 \times 10^{14}/\text{cm}^2$ ), the  $[Zr(MNV)+S(LMM)]/Zr(MNN)$  ratio changes as a function of sputtering time for three Ar-ion beam energies of 1, 2, and 3 keV. The size of the rectangle enclosing the initial data points for the three cases indicates the uncertainty in these measurements. Regardless of ion beam energy the  $[Zr(MNV)+S(LMM)]/Zr(MNN)$  ratio rapidly drops for the first several minutes and is then affected very little. Within the experimental uncertainty of our experi-

ments it is difficult to distinguish the three cases. This observation may be especially relevant for studies of zirconium single crystals where there is a desire to reduce ion beam damage during cleaning to a minimum. Since there is no significant difference in cleaning the surface of sulfur using 1 or 3 keV one can use lower beam energies and thus reduce damage to the surface structure.

Zry-4 is used as a structural material in nuclear reactors where its mechanical properties combined with low neutron absorption cross section and corrosion resistance play essential roles. However, the surface chemistry of this alloy under UHV conditions has not been extensively studied in the past. Our main interest is to investigate surface oxidation in the presence of sulfur, which can be present as an impurity. We showed earlier how the surface of this alloy oxidizes after oxygen<sup>9</sup> and water<sup>16</sup> adsorption. Here we show how sulfur dioxide chemisorption also results in surface oxidation. Our findings are interesting since sulfur was previously found to delay surface oxidation<sup>10</sup> and reduce the sticking coefficient of adsorbing oxygen<sup>17</sup> on zirconium surfaces.

#### IV. SUMMARY

After  $\text{SO}_2$  adsorption on Zry-4 at 300 K the  $Zr(MNN)$  feature shifts toward lower energies by about 3 eV, indicating surface oxidation by dissociated oxygen. Temperature programmed desorption experiments are consistent with dissociation of  $\text{SO}_2$  as no molecular desorption was observed. Relatively short Ar-ion sputtering removes sulfur from the near-surface region without significantly affecting the oxygen Auger signal. After annealing the  $\text{SO}_2/\text{Zry-4}$  system sulfur remains near the surface, whereas oxygen is dissolved into the bulk.

<sup>1</sup>V. E. Henrich and P. A. Cox, *The Surface Science of Metal Oxides* (Cambridge University, Cambridge, 1993).

<sup>2</sup>D. A. Outka and R. J. Madix, *Surf. Sci.* **137**, 242 (1984).

<sup>3</sup>J. Ahner, A. Effendy, K. Vajen, and H.-W. Wassmuth, *Vacuum* **41**, 98 (1990).

<sup>4</sup>N. Stojilovic, J. C. Tokash, and R. D. Ramsier, *Surf. Sci.* **553**, 23 (2004).

<sup>5</sup>P. C. Wong and K. A. R. Mitchell, *Can. J. Chem.* **64**, 23 (1986).

<sup>6</sup>Y. C. Kang, M. M. Milovancev, D. A. Clauss, M. A. Lange, and R. D. Ramsier, *J. Nucl. Mater.* **281**, 57 (2000).

<sup>7</sup>N. Stojilovic, J. C. Tokash, and R. D. Ramsier, *Surf. Sci.* **565**, 243 (2004).

<sup>8</sup>N. Stojilovic, E. T. Bender, and R. D. Ramsier, *Appl. Surf. Sci.* **252**, 1806 (2005).

<sup>9</sup>N. Stojilovic, E. T. Bender, and R. D. Ramsier, *J. Nucl. Mater.* **348**, 79 (2006).

<sup>10</sup>T. Tanabe and M. Tomita, *Surf. Sci.* **220**, 333 (1989).

<sup>11</sup>J. Ahner, A. Effendy, and H.-W. Wassmuth, *Surf. Sci.* **269/270**, 372 (1992).

<sup>12</sup>M. Yamamoto, C. T. Chan, K. M. Ho, and S. Naito, *Phys. Rev. B* **54**, 14111 (1996).

<sup>13</sup>Y. M. Wang, Y. S. Li, and K. A. R. Mitchell, *Surf. Sci.* **343**, L1167 (1995).

<sup>14</sup>K. Griffiths, *J. Vac. Sci. Technol. A* **6**, 210 (1988).

<sup>15</sup>C.-S. Zhang, B. Li, and P. R. Norton, *Surf. Sci.* **346**, 206 (1996).

<sup>16</sup>N. Stojilovic and R. D. Ramsier, *Appl. Surf. Sci.* (in press).

<sup>17</sup>K. Ojima and K. Ueda, *Appl. Surf. Sci.* **165**, 141 (2000).